Orientation of Polymer Coils in Dilute Solutions Undergoing Shear Flow: Birefringence Experiments

Jacques Bossart and Hans Christian Öttinger*

Department of Materials, Institute of Polymers, ETH Zürich, and Swiss F.I.T. Rheocenter, CH-8092 Zürich, Switzerland

Received March 11, 1997; Revised Manuscript Received June 12, 1997[⊗]

ABSTRACT: Polymer orientation in dilute solutions undergoing shear flow is investigated by means of flow birefringence using a quantity called "orientation resistance". In the framework of theoretical models it was found that the intrinsic orientation resistance is strongly influenced by polydispersity (Bossart and Öttinger, 1985). Dilute solutions of two radical polymerized polystyrene samples with different molecular weights in both good and Θ solvents are investigated by flow birefringence. The experimentally obtained values for the intrinsic orientation resistance are in very good agreement with the values calculated in the framework of kinetic polymer models. These experiments demonstrate that the polydispersity effect is well understood and that flow birefringence constitutes an extremely precise method for determining molecular weights. From our experiments it can be inferred that the number-average molecular weight M_n of a polymer sample can be measured to within a relative error of $\Delta M_n/M_n = 3\%$. The use of the birefringence method for the determination of the molecular weight distribution of a polymer sample is suggested.

1. Introduction

The orientation of polymers can be determined by flow birefringence, by scattering methods such as light scattering or neutron scattering, or by translational diffusion. However, these orientation angle measurement techniques are fundamentally different. It was shown in ref 1 that different measurement results are expected due to the different length scales involved in the individual techniques.

Flow birefringence as a method for determining orientation angles of polymers in solution or in a melt was developed by Tsvetkov[2] and Janeschitz-Kriegl[3,4] in the 1950s and 1960s. The main purpose of these works was to construct an apparatus able to measure orientation angles χ_τ of polymers at low reduced shear rates $\beta < 1$. Indeed, with an apparatus built by Janeschitz-Kriegl,[3] reliable orientation angle experiments became possible at a very small flow birefringence of $\Delta n = 10^{-8}$. This could be realized by avoiding the disturbing influence of parasitic double refraction. It is the original appartus which is used in the present work.

Despite the fact that the technique was fully developed 20 years ago, little experimental attention has been focused on the influence of polydispersity on orientation angle measurements. The so-called "orientation resistance" is a suitable quantity to investigate the orientational behavior of polymers and the influence of polydispersity. In a previous paper,[1] we discussed the concept of the orientation resistance for different measurement techniques. It is a dimensionless quantity and becomes universal in the limit of vanishing shear rates; therefore, it does not depend on chemical details of the polymer. Werner Kuhn,[5] who introduced the random coil model for dilute polymer solutions, noticed in one of his landmark papers that the molecular weight of a polymeric system can be determined from the combination of orientation angle and viscosity measurements. Apart from that he realized that this procedure is free of assumptions about the monomers. Since it can be derived directly from the orientation angle curves, the orientation resistance values obtained theoretically in the framework of kinetic models can easily be compared to experimental results.

In section 2 we summarize the theoretical findings for the orientation resistance and motivate the experimental verification of the strong polydispersity effect. The flow birefringence apparatus and its properties, as well as the polydisperse polymers and solvents, are discussed in section 3. In section 4 we present the orientation angle and flow birefingence results and discuss them in the context of the orientation resistance concept. Then, we compare the experimental values to the theoretical ones and show that the predicted polydispersity effect is correct. In particular, we present a thorough error analysis of the orientation angle measurement and give an estimate of the accuracy of the molecular weight determination with this method.

2. Theory

2.1. Flow Birefringence and the Stress−Optical Law. The flow birefringence of polymer solutions has two origins: form birefringence and intrinsic birefringence. The former is connected with the anisotropy in the correlation of the segment density. If the global shape of the polymer is altered from a sphere to an anisotropic shape, form birefringence arises if the refractive indices of the solvent and the solute are different. The origin of intrinsic birefringence lies in the anisotropic polarizability of the segments. If the conformation of the chain is altered, then the local anisotropy leads to a macroscopic anisotropy.

The orientation of polymers is characterized by the orientation angle which, in simple shear flow, is the angle between the flow direction and the larger principle axis of the sectional ellipse of the refractive index ellipsoid (associated with the refractive index tensor) in the plane of shear.

Unfortunately, the flow birefringence of a polymer solution is a superposition of both contributions, intrinsic and form birefringence. The latter one is a rather complicated effect and can be connected with the form factor[6] arising in the light intensity scattered by the macromolecules. Form birefringence is based on the long-range dipole−dipole interaction of different chain

* To whom correspondence should be addressed.
[⊗] Abstract published in *Advance ACS Abstracts,* August 1, 1997.

S0024-9297(97)00328-8 CCC: $14.00

segments which leads to an additional anisotropy of the polymers.[7] Here, it is particularly important to note that the fundamental quantity entering the calculation is the mean excess polarizability of the solution and therefore the increment of the refractive index with decreasing polymer concentration c_p, namely $dn/dc_p = \lim_{c_p \to 0}(n - n_0)/c_p$ (n_0 is the refractive index of the pure solvent, and n denotes the refractive index of the solution), so that the intrinsic anisotropy of the segments can be neglected for this effect. This is basically the reason why the total birefringence can be written as the sum of both effects, which has been proven at least for the case of flows with small shear rates.[8] Usually, the form birefringence is suppressed by choosing the solvent and the solute to be isorefractive.

The anisotropic refractive index tensor arising from intrinsic birefringence can be related to the stress tensor. The so-called stress−optical law states that the anisotropic intrinsic part of the refractive index tensor is proportional to the anisotropic stress tensor. This relation can be derived theoretically under the assumption of Gaussian statistics of the segments of the (necessarily very long) polymer chain. Second, the additivity of the segment polarizabilities is assumed.[6] The stress−optical law has been found to hold for rubbers and generally for polymeric liquids.[3,4] The only explanation for such a general relation is that both stress and birefringence have the same physical origin, i.e. orientational ordering on a scale small compared to the entire polymer coil but large compared to the monomer.

2.2. Orientation Resistance. In the following we give an overview of the orientation resistance concept and summarize the results obtained in ref 1 necessary for a comparison to the experiments.

In flow birefringence experiments the orientation angle of the polymer chains is defined by the measured extinction angle. According to the stress−optical law, this angle can be identified with the orientation angle of the sectional ellipse of the stress ellipsoid in the plane of shear relative to the flow direction. Hence, we can write down the following relation, where the second part serves as a definition of the orientation resistance $m_\tau(\beta)$

$$\tan 2\chi_\tau = \frac{2\tau_{21}}{\tau_{11} - \tau_{22}} \equiv \frac{m_\tau(\beta)}{\beta} \tag{1}$$

Here, χ_τ is the orientation angle measured by flow birefringence, τ_{jk} are the components of the stress tensor, and the dimensionless quantity β is the reduced shear rate $\beta \equiv ([\eta]_0\eta_s M/RT)\dot\gamma$ with $[\eta]_0 \equiv \lim_{\dot\gamma\to 0}\lim_{c_p\to 0}\eta_p/c_p\eta_s$ ($\dot\gamma$, time-independent shear rate; c_p, polymer concentration; $[\eta]_0$, zero-shear-rate intrinsic viscosity; η_s, solvent viscosity; η_p, polymer contribution to the viscosity of the solution at concentration c_p; M, molecular weight of the polymer; R, universal gas constant; T, absolute temperature). The quantity $[\eta]_0\eta_s M/RT$ is a characteristic time constant for the polymer solution suggested by molecular theories.[10] In ref 1 it was argued that the name orientation resistance can be motivated by the fact that in linear viscoelastic models the inverse of the intrinsic orientation resistance (the orientation resistance in the limit of vanishing shear rate) is the reduced steady-state compliance.

The intrinsic orientation resistance of polymers undergoing simple shear flow, m_τ^0, was calculated and discussed in ref 1 in the framework of bead-spring models for linear polymers in a Θ solvent, namely for the Rouse model[11] and, including hydrodynamic interaction, for the Zimm model,[12,13] the Gaussian approximation,[14,15] and the renormalization group method.[16,17] Simple shear flow is characterized by the velocity gradient tensor κ

$$\boldsymbol{v}(\boldsymbol{r}) = \boldsymbol{v}_0 + \kappa\cdot\boldsymbol{r}, \quad \kappa = \begin{pmatrix} 0 & \dot\gamma & 0 \\ 0 & 0 & 0 \\ 0 & 0 & 0 \end{pmatrix} \tag{2}$$

In the orthogonal laboratory system, direction 1 is that of the streamlines and direction 2 is that of the velocity gradient. Plane 1,2 is the plane of flow, and direction 3 is normal to this plane.

Table 1. Orientation Resistance for the Stress Tensor in the Rouse and Zimm Models, the Gaussian Approximation, and the First-Order Perturbation Theory Refined by the Renormalization Group Method (RG)[a]

m	Rouse	Zimm	Gauss	RG
m_τ^0	2.50	4.832	3.57(2)	3.28

[a] The m_τ^0-values for the Zimm model and the RG-approximation can be derived directly from results in refs 13 and 17.

Since hydrodynamic interaction is neglected in the Rouse model, we cannot expect realistic results from that model. In the Zimm model, hydrodynamic interaction is included in a preaveraged form,[10] whereas in the Gaussian approximation and in the refined perturbation theory, fluctuations are taken into account. Therefore, the last two approximations are considered as the best analytical tools for the calculation of rheological quantities of dilute polymer solutions. The orientation resistance results in Table 1 associated with flow birefringence show that indeed the hydrodynamic interaction is an important effect. While the Zimm model seems to overestimate hydrodynamic interaction, the Gaussian approximation and the refined perturbation theory values for the orientation resistance are reasonably close together. Therefore, we anticipate that these two values will give the best comparison to experimental data. Further, it was argued in ref 1 that the orientation resistance is only slightly affected by the excluded volume effect,[17] which is not included in our results presented in Table 1; therefore, our values can be compared to experimental results in both Θ and good solvents.

The polydispersity of a polymer sample is taken into account by properly averaging the components of the stress tensor in eq 1. The orientation angle of a polydisperse polymer system at low reduced shear rates can be written as[1]

$$\chi_\tau = \frac{\pi}{4} - \frac{1}{2}\frac{1}{m_\tau^0 p_\tau}\beta_n \quad \text{with} \quad p_\tau = \frac{\langle\langle M^b\rangle\rangle_n^{\,2}}{\langle\langle M^{2b}\rangle\rangle_n} \tag{3}$$

The quantity m_τ^0 is the orientation resistance in the limit of vanishing shear rate, p_τ is called the polydispersity factor, and the brackets $\langle\langle\cdot\rangle\rangle_n$ denote a number-average quantity. It gives a measure for the polydispersity effect. The product $m_\tau^0 p_\tau$ can be understood as the orientation resistance of the polydisperse system. The polydispersity factor takes values between zero and one. For a strictly monodisperse system, $p_\tau = 1$, and the more polydisperse a system is the smaller p_τ becomes. For the derivation of the polydispersity factor in eq 3 appropriate scaling laws for the molecular weight dependence of the stress tensor components are as-

Table 2. Exponents ν and b for the Free Draining Case (Rouse), in the Presence of Hydrodynamic Interaction Only (HI), and with Hydrodynamic Interaction and Excluded Volume (HI, EV)

	Rouse	HI	HI, EV
ν	1/2	1/2	0.588(1)
b	2	3/2	1.764(3)

sumed.[1] The values for the exponent b are given in Table 2. The increase in the exponent b means that the polydispersity effect is increased by the excluded volume effect.

The average reduced shear rate $\beta_n \equiv (\langle\langle[\eta]_0\rangle\rangle\ \eta_s M_n/RT)\ \dot{\gamma}$ contains average quantities such as the number-average molecular weight M_n and the average intrinsic viscosity $\langle\langle[\eta]_0\rangle\rangle$ defined as

$$\langle\langle[\eta]_0\rangle\rangle \equiv \lim_{\dot{\gamma}\to 0}\lim_{c_p\to 0}\frac{\eta_p(M_0)}{\eta_s c_p(M_0)}M_0^{1-b}\frac{\langle\langle M^b\rangle\rangle_n}{\langle\langle M\rangle\rangle_n} \qquad (4)$$

Here, the polymer contribution to viscosity $\eta_p(M_0)$ and the polymer concentration $c_p(M_0) = n_p M_0/N_A$ (n_p, polymer number density; N_A, Avogadro's number) are both evaluated for the same polymer system at a fixed reference molecular weight M_0. The average expression in the numerator of eq 4 accounts for the viscosity of a polydisperse system, and the average expression in the denominator accounts for the weighing process of a certain amount of a polydisperse polymer.

In ref 1 it was shown for the case of a Schulz−Zimm and a logarithmic-normal molecular weight distribution that the polydisperse orientation resistance $m_\tau^0 p_\tau$ is very sensitive to the polydispersity M_w/M_n and to the type of molecular weight distribution.

From a plot of the orientation angle χ_τ against the average reduced shear rate β_n, the experimental value for the polydisperse orientation resistance $m_\tau^0\ p_\tau$ is obtained from the initial slope of the curve. This value can then be compared to the theoretical value m_τ^0 or it can be compared to other measurements with the help of the polydispersity factor p_τ:

$$m_\tau^0(p_\tau(1)) = \frac{p_\tau(1)}{p_\tau(2)}m_\tau^0(p_\tau(2)) \qquad (5)$$

If, for example, the orientation resistance $m_\tau^0(p_\tau(1))$ of system 1 and $p_\tau(1)$ are known, then the polydispersity factor $p_\tau(2)$ for system 2 can be predicted from eq 5 after a measurement of the orientation resistance $m_\tau^0(p_\tau(2))$.

Equation 5 will be employed in section 4 to reduce the experimentally determined orientation resistances for polydisperse polymer systems to the corresponding monodisperse values so that they can be compared among each other and to the theoretical values (which are calculated for monodisperse polymers).

3. Experimental Arrangement and Materials

3.1. Apparatus. The apparatus used in this work for the determination of the extinction angle and the flow birefringence of dilute polymer solutions was built by H. Janeschitz-Kriegl[3] at the Central Laboratory TNO in Delft, The Netherlands, at the end of the 1960s. The rotor unit itself can still be considered as one of the most thorough constructions of its kind. With the present apparatus measurements are possible down to a birefringence of $\Delta n = 1 \times 10^{-8}$. The apparatus is described in detail in refs 3 and 18−23.

All measurements of this work were carried out with the rotor unit and the optical alignment in its original form, whereas the drive, its control system, and the heating system have been replaced.

The unit, which is of a Searle type, has a rotating internal cylinder (radius = 2.5 cm, height = 5 cm) whereas the external cylinder serves as stator. The gap width is 0.25 mm. The cylinders are made of black glass NG1, Schott & Gen., and have carefully polished surfaces. A high-pressure mercury lamp is used as light source. Glan-Thompson prisms were chosen for the polarizer and the analyzer. From the viewpoint of geometrical optics the optical alignment is adjusted such that the light beam is leaving the annular gap without being reflected at the cylinder walls.[3] However, when the light enters the annular gap diffraction occurs. Only the light which is of zeroth order in the diffraction pattern propagates through the gap without being reflected at the cylinder walls. The light corresponding to higher orders is reflected and is therefore phase shifted. It is found experimentally that, with crossed prisms, only the zeroth order is extinguished.[22] The disturbing influence of the diffraction pattern can be avoided by the introduction of a slit in front of the ocular.

The light is entering and leaving the rotor unit through two windows at the bottom and the top of the unit. The construction of the windows is of particular interest. They are cuvettes, made of one piece of glass (BK7, Schott & Gen.), with a flat bottom which is polished on both sides. In order to avoid extra strains in the windows due to temperature fluctuations, the windows are not directly cemented in the rotor unit but fit slidingly in a fitting. The sealing of the windows is achieved by a thin silicone oil layer between the fitting and the window. In both cases the fluid in the rotor unit is prevented from reaching the silicone oil by an air cushion between the fluid and the silicon oil layer. Teflon rings serve for a seal between the fitting and the bottom (top) of the rotor unit.

In this way, both windows remain revolvable by rotating their fittings in the rotor unit, and therefore, the small strain birefringence of the windows can be compensated with a weakly birefringent compensator plate once for all by gauging the apparatus properly.[24]

From various experimental investigations the conclusion could be drawn that a nonabsorbant medium (glass) as a material for the rotor and the stator is to be preferred over metal.[22] There are two reasons for this. First, metal walls tend to cause severe phase shifts in the light reflected at the walls, whereas walls made of glass lead to smaller phase shifts. Second, the amount of light reflected at the walls can be minimized by making sure that the light beam propagates undisturbed through the annular gap. This can be achieved by avoiding a radial temperature gradient. Although the high conductivity of metal walls has the advantage of removing the frictional heat, it is responsible for the formation of such an undesired nonuniform temperature distribution in the gap. It was shown by model calculations[23] that an insulator such as glass leads to a uniform temperature distribution if the frictional heat is removed by means of a circulation stream through the annular gap. This additional superimposed flow in the 3,2-plane is produced in our apparatus by a screw pump attached at the bottom of the rotor. In order to avoid a

measurable disturbance of the orientation angle and birefringence measurements by the extra convection stream, the largest velocity gradient of the stream, which occurs near the cylinder walls, was chosen to be only one-tenth of the velocity gradient of the main shear flow.

A theoretical estimation of the effect of this extra stream on the orientation resistance in the framework of kinetic models gives a valuable insight. Since the annular gap is very small compared to the radius of the cylinders we assume that the axial flow is a Poiseuille-type flow as it occurs between two parallel plates. In the middle of the gap the contribution to shear from this flow is zero, whereas it becomes maximum at the walls. We study the influence of the superimposed axial flow by introducing an adjustable shear rate in the 3,2-plane proportional to the applied shear rate $\dot{\gamma}$ of the main flow. The velocity field then is characterized by

$$\kappa = \begin{pmatrix} 0 & \dot{\gamma} & 0 \\ 0 & 0 & 0 \\ 0 & \mu\dot{\gamma} & 0 \end{pmatrix} \tag{6}$$

The coordinate system is the same as in section 2.2. The parameter μ measures the strength of the axial current relative to the applied shear rate $\dot{\gamma}$ of the main flow ($-1 < \mu < +1$). For our apparatus the parameter μ equals $\mu = {}^1/_{10}$. An analytical consideration in the Rouse model shows that the extra stream in the 3,2-plane has no influence on the shear stress and the first normal stress difference and hence on the orientation resistance m_τ.[24] However, the Rouse model does not include hydrodynamic interaction and is not very typical for a dilute polymer solution. A Brownian dynamic simulation for polymer chains with $N = 10$ beads in a Θ solvent including hydrodynamic interaction was therefore performed for the velocity field defined in eq 6 with $\mu = {}^1/_{10}$. Hydrodynamic interaction was treated by the Rotne−Prager tensor, and the hydrodynamic interaction parameter was chosen to be $h^* = 0.15$. The influence of the superimposed flow was studied at reduced shear rates $\beta = 1.3$, 8.2, 27.4, and 137.3. The steady state simulations were performed with an Euler scheme for different time steps and a time step extrapolation.[25] The results for the orientation resistance with and without extra stream were in perfect agreement within the statistical error bar of about 2%.[24] We hence conclude that the extra convection stream in the 3,2-plane does not disturb the orientation angle measurement in the 1,2-plane.

The extinction angle (the orientation angle of the polymers) is measured by rotating together the (crossed) polarizer and analyzer until maximum attenuation is obtained. The flow birefringence is determined by the de Sénarmont method:[26] a $\lambda/4$-plate, which transforms the elliptical light into linearly polarized light again,[26] is installed in the light path after the birefringent material in front of the analyzer. First, the polarizer and the analyzer have to be crossed. Then the $\lambda/4$-plate is mounted in a fitting in front of the analyzer and revolved such that the alignment of its principle axes coincides with the one of the polarizer and the analyzer (extinction must be obtained). In a next step the polarizer−$\lambda/4$-plate−analyzer system is rotated by 45° relative to the previously determined extinction position of the birefringent medium. Then, we measure the phase shift by rotating the analyzer by the angle Φ until extinction of the linearly polarized light occurs again. The angle of rotation Φ is directly connected to the birefringence by

$$\Delta n = \frac{\lambda_0}{\pi d_r}\Phi \tag{7}$$

where λ_0 denotes the wave length of the light (in our case the green line of a mercury lamp at 546 nm) and d_r is the height of the rotor ($d_r = 50$ mm). The accuracy of this method is of the order of $\delta(\Delta n) = \pm 10^{-8}$ for our apparatus.[26]

3.2. Materials. The molecular weight of polymeric systems best suited for the exact measurement of the orientation resistance has a lower and an upper limit. From the definition for the reduced shear rate β and the stress−optical law the following equations can be derived

$$\Delta n_1 = \frac{2c_p C\beta RT}{M}\frac{1}{\sin 2\chi} \tag{8}$$

$$= 2n_p C\beta k_B T \frac{1}{\sin 2\chi} \tag{9}$$

Here, Δn_1 denotes the polymer contribution to the birefringence, C is the stress−optical coefficient, and k_B is the Boltzmann constant. The expression $\sin 2\chi$ only depends on molecular weight through the reduced shear rate β. For fixed values β and c_p the birefringence Δn_1 is therefore inversely proportional to the molecular weight M. Since we are dealing with dilute solutions, the polymer number density n_p must become very small when the molecular weight M is increased to large values. We conclude that the polymer contribution to flow birefringence becomes smaller when the molecular weight is increased. For a precise determination of the orientation resistance the experiments should be carried out with polymer samples of not too high molecular weights. This conclusion has already been drawn in ref 3. A lower limit of molecular weight is given by the requirement that the polymers must form statistical coils. Although in this work we are not interested in the high β-regime, we note that, for decreasing molecular weight M, the shear rate $\dot{\gamma}$ needed for the achievement of a certain β-value is increasing. Thus, flow instabilities at high shear rates will limit the lower limit of molecular weight that can be examined. The use of a more viscous solvent can then help shift the reduced shear rate β to higher values.

Since we want to avoid form birefringence in the experiments, the refractive index of the solvent has to match that of the polymer (low refractive index increment). It was found experimentally by Tsvetkov[2] that a refractive index increment of less than 0.1 cm^3/g has no detectable effect on steady flow birefringence experiments for dilute solutions. Additionally, the solvent is expected to have a low proper flow birefringence in order to have no solvent influence on the actual flow birefringence measurement. Unfortunately, these solvent properties cannot all be achieved in an ideal way.

The theoretical considerations in the framework of kinetic models assume linear polymers in a Θ solvent. We realize such a system by using 4-bromo-α-methylbenzyl alcohol (Aldrich, Buchs, lot BQ07501TN) as a solvent and radical polymerized polystyrene samples with different molecular weights. It was reported in ref 3 that this solvent is a Θ solvent for polystyrene at $T =$ 18 °C. The melting point of our solvent is $T = 36$ °C, and we were not able to undercool the liquid down to T

Table 3. Characterization Data for the Investigated Radical Polymerized Polystyrene and for the Solvents Used[a]

				intrinsic viscosities (cm^3/g)	
	$10^{-5}M_n$	$10^{-5}M_w$	M_w/M_n	bromobenzene, 25 °C	4-bromo-α-methylbenzyl alcohol, 35 °C
PSBR14125	2.89	5.12	1.77	172.9	35.9 ± 3.6
PSBR240k	1.41	2.40	1.70	92.9	23.6 ± 2.4
PSBR240k/PSBR14125	1.74	3.38	1.94	123.7	27.6 ± 2.8
viscosity (poise)				0.0105	0.1735
density (g/cm^3)				1.4882	1.4475

[a] The molecular weight data are extracted from the numerical GPC-curves shown in Figures 1 and 2. The viscosity, the intrinsic viscosity, and the density values were measured as explained in the text except the viscosity and the density data of bromobenzene which come from ref 3. The ratio of the weight fractions for the mixture is PSBR240k:PSBR14125 = 0.64:0.36.

= 18 °C. Instead we performed our measurements at T = 35 °C. The authors believe that the solvent used in ref 3 was not as pure as it was in our case (gas liquid chromatography: 97.1%). Nevertheless, an investigation of the experimental results presented in ref 3 shows that the Mark Houwink exponents from intrinsic viscosity on narrowly distributed polystyrenes with different molecular weights ($M_w = 2.24 \times 10^5$ and $M_w = 1.59 \times 10^6$) varies between 0.49 and 0.52 when going from T = 18 °C to T = 40 °C. Since the polymer samples used in the present work (see below) have molecular weights lying within this range, we conclude that our solutions of polystyrene in 4-bromo-α-methylbenzyl alcohol at T = 35 °C can still be considered as near-Θ solutions.

We use bromobenzene as a good solvent at T = 25 °C. Bromobenzene has been widely used as a good solvent for polystyrene[2,3] in flow birefringence measurements.

Fortunately, both liquids show a rather small refractive index increment with polystyrene,[3] namely dn/dc_p = 0.046 cm^3/g (bromobenzene, T = 25 °C) and dn/dc_p = 0.055 cm^3/g (4-bromo-α-methylbenzyl alcohol, T = 18 °C). Thus, form birefringence can be neglected in both cases.

The measurement of absolute viscosity of 4-bromo-α-methylbenzyl alcohol was performed with an Ubbelhode-viscometer (Type 0a, Schott, Mainz, Germany) using standard methods (temperature control ±1/20 °C). The error is estimated to be less than 1% and is therefore neglected in the subsequent calculations. The results are displayed in Table 3.

The polystyrene samples were synthesized and characterized by Polymer Standards Service GmbH, Mainz, Germany. They were polymerized in bulk and the characterization was performed by means of GPC, using a traditional calibration curve (polystyrene standards). The samples PSBR14125 and PSBR240k are radical polymerized polystyrenes with relatively low conversion rates (PSBR14125: < 10%; PSBR240k: < 20%). The average molecular weights M_n, M_w and the polydispersity M_w/M_n are displayed in Table 3. They were calculated by using the GPC curves in Figures 1 and 2.

As the samples were polymerized in bulk only chain transfer from initiator molecules or from monomers to the end of the growing chain can occur. The first case leads to a widening of the mass distribution function; a theoretical consideration shows that the polydispersities of the samples should lie between 1.5 and 2.0 and they indeed do so (see Table 3). The second case is connected to chain branching. The number of branching points depends on the conversion rate of monomers and on the transfer constant. It can be estimated[24] that one in 35 polymers is branched in our systems. From that we consider our systems to be consisting of linear polymers.

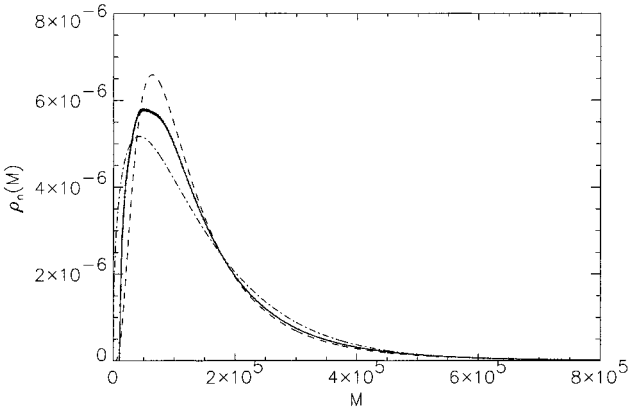

Figure 1. Molecular weight distribution function (solid line) extracted from a GPC characterization of PSBR240k. Here, $\rho_n(M)dM$ is the number fraction of molecules with molecular weights between M and $M + dM$. The dashed line is the logarithmic-normal distribution and the dashed−dotted line denotes the Schulz−Zimm distribution calculated with the average molecular weights obtained from the GPC curve.

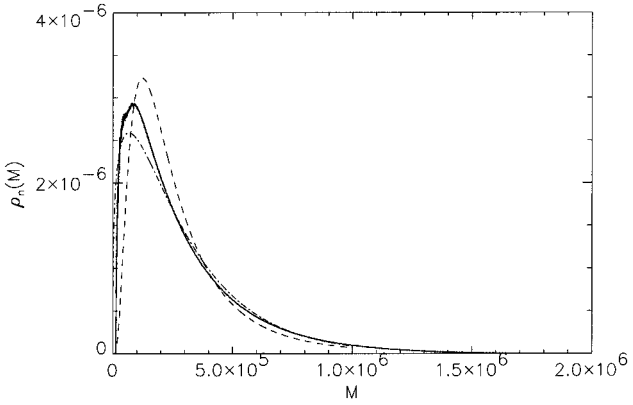

Figure 2. Molecular weight distribution function (solid line) extracted from a GPC characterization of PSBR14125. Here, $\rho_n(M)dM$ is the number fraction of molecules with molecular weights between M and $M + dM$. The dashed line is the logarithmic-normal distribution and the dashed−dotted line denotes the Schulz−Zimm distribution calculated with the average molecular weights obtained from the GPC curve.

The molecular weights of these samples are very suitable for our experimental purpose (see Table 3): high enough such that the polymers can be considered as statistical coils and small enough to enable precise experiments (section 4).

Theoretically, the described polymerization process should lead to the so-called Schulz−Zimm molecular weight distribution function. However, the GPC-curves in Figures 1 and 2 deviate from the corresponding Schulz-Zimm distribution functions. The maximum is shifted slightly toward higher molecular weights. The so-called Trommsdorff-effect (gel-effect) could be respon-

Table 4. Typical Overlap Concentrations c_p^* for Polymer Systems with the Indicated Molecular Weights

$10^{-5}M_w$	[Θ solvent] (g/100 mL)	[good solvent] (g/100 mL)
5.12	1.90	0.80
2.40	2.80	1.40

sible for that, in particular because it is known to become important when polymerization takes place in bulk. As a consequence, we refer directly to the GPC-mass-distribution function and not to the Schulz−Zimm distribution in our experiments. On the other hand, we are aware of the fact that GPC is not a very precise measurement technique. We estimate the errors in the average molecular weights to be 10%.

The intrinsic viscosities of the polystyrene samples in bromobenzene were measured with an automatic capillary viscometer constructed at the Institute for Polymers, ETH Zürich, whereas the ones in 4-bromo-α-methylbenzyl alcohol were measured with a capillary viscometer of a Cannon−Fenske-type. The concentrations used were significantly lower than the estimated overlap concentrations, which are displayed in Table 4. They were calculated under the assumption of a typical radius of gyration ($\sqrt{R_G^2}$ = 220 Å/300 Å for PSBR-14125 in a Θ/good solvent, $\sqrt{R_G^2}$ = 150 Å/190 Å for PSBR240k in a Θ/good solvent) according to the formula

$$c_p^* = \frac{M}{N_A \frac{4}{3}\pi R_G^3} \propto M^{1-3\nu}, \qquad (10)$$

where the exponent ν is displayed in Table 2. The viscosity data were linearly extrapolated to zero concentration. The quoted errors of the intrinsic viscosities in 4-bromo-α-methylbenzyl alcohol can be explained as follows: each concentration (of four) was measured separately. The volume of each solution was 10 mL. The production of the individual concentrations as well as the determination of the elution time involve errors which we estimate to be 10% of the absolute value of the intrinsic viscosities. On the other hand, since the measurements in bromobenzene are run automatically, each step and also the extrapolated results involve negligible errors.

In order to examine the theoretical predictions for the polydispersity corrections we want to mix both systems, namely PSBR14125 and PSBR240k, such that the polydispersity effect on the orientation resistance is maximized. The advantage of such a procedure compared to the usage of a polydisperse technical polymer system is given on the one hand by the reliable determination of polydispersity and on the other hand by the absence of branching. Of course, the polydispersity obtainable from such a mixture is relatively small. Now, we are free to choose the weight fractions of both components, in order to minimize the polydispersity factor p_τ and, by that, to maximize the polydispersity effect. If we assume that our systems can be described adequately with the two Schulz−Zimm distribution functions displayed in Figures 1 and 2 and we minimize the polydispersity factor for the case of a good solvent, we obtain the following ratio of weight fractions PSBR240k:PSBR14125 = 0.64:0.36. This ratio will be used for the mixture in the orientation angle measurements. The resulting mixture of the GPC curves in Figures 1 and 2 then leads to the polydispersity factors displayed in Table 5 and to the average molecular weights shown in Table 3. Although the mixing ratio was determined for good solvents, we take the same rule for the experiments in the Θ solvent. In Table 5 we also display the polydispersity correction factors for the systems PSBR240k and PSBR14125.

Table 5. Polydispersity Correction Factors for the Indicated Radical Polymerized Polystyrenes[a]

	polydispersity factors p_τ	
	bromobenzene	4-bromo-α-methylbenzyl alcohol
PSBR240k	0.246	0.341
PSBR14125	0.270	0.350
PSBR240k/PSBR14125	0.179	0.263

[a] The data are extracted from the GPC curves shown in Figures 1 and 2. The ratio of the weight fractions for the mixture is PSBR240k:PSBR14125 = 0.64:0.36.

3.3. Correction for the Influence of the Flow Birefringence of the Solvent. The birefringence and extinction angle measured in a flow birefringence experiment on dilute polymer solutions are always results of a two-component system, namely the solvent molecules and the polymers. Since we are interested only in the properties of the polymers the influence of the solvent molecules has to be subtracted from the measured quantities.

The solvent molecules are usually very small compared to the length scale of the polymers and the time scale on which the fluid is subjected to shear in typical flow birefringence experiments is much larger than the characteristic relaxation time of the solvent molecules. The net orientation of the solvent molecules, when subjected to shear, will always be at an angle of $\pi/4$ relative to the direction of flow. For polymers on the other hand, the orientation depends strongly on the shear rate applied, decreasing toward zero for values of $\beta > 1$.

We assume now that the index tensors of the two components are additive. Transforming both tensors to the laboratory system (defined in section 2.2), adding them, and diagonalizing the resulting tensor leads to the formulas

$$\tan 2\chi = \frac{\Delta n_1 \sin 2\chi_1 + \Delta n_2 \sin 2\chi_2}{\Delta n_1 \cos 2\chi_1 + \Delta n_2 \cos 2\chi_2} \qquad (11)$$

$$\Delta n^2 = (\Delta n_1 \sin 2\chi_1 + \Delta n_2 \sin 2\chi_2)^2 + (\Delta n_1 \cos 2\chi_1 + \Delta n_2 \cos 2\chi_2)^2 \qquad (12)$$

where χ, χ_1, and χ_2 denote the orientation (extinction) angles of the two component system, the polymers and the solvent molecules respectively. The birefringences Δn, Δn_1, and Δn_2 are defined in the same way.

These equations can be solved for χ_1 and Δn_1. If we additionally set $\chi_2 = \pi/4$ we obtain

$$\tan 2\chi_1 = \frac{\Delta n \sin 2\chi - \Delta n_2}{\Delta n \cos 2\chi} \qquad (13)$$

$$\Delta n_1^2 = \Delta n^2 + \Delta n_2^2 - 2\Delta n \Delta n_2 \sin 2\chi \qquad (14)$$

Equations 11 and 12 have been elaborated already in ref 27, where the polarizability of a multicomponent liquid was studied. However, the approach was not a geometrical one and was far more complicated than the one given here. In the next section we will use eqs 13

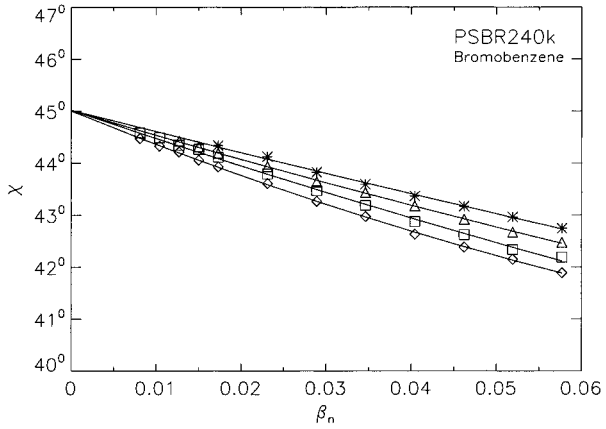

Figure 3. Orientation angle χ as a function of the reduced average shear rate β_n for polystyrene PSBR240k in bromobenzene at the concentrations 1.25 (◇), 1.00 (□), 0.75 (△), and 0.50 g/100 mL (∗). All values are corrected according to eq 13.

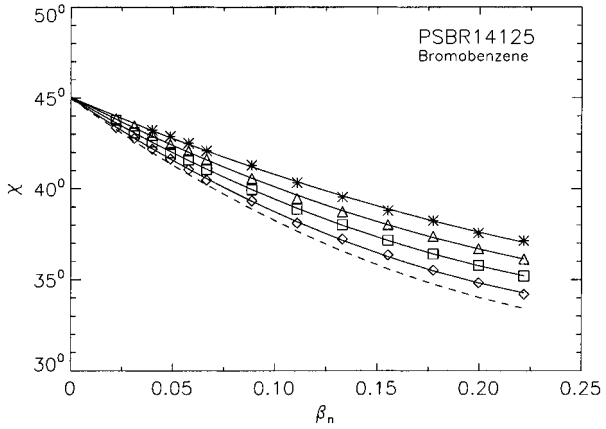

Figure 4. Orientation angle χ as a function of the reduced average shear rate β_n for polystyrene PSBR14125 in bromobenzene at the concentrations 1.25 (◇), 1.00 (□), 0.75 (△), and 0.50 g/100 mL (∗). All values are corrected according to eq 13. The uncorrected values for the highest concentration are plotted as a dashed line.

and 14 to correct the measured orientation angle values and the birefringence data.

4. Experimental Results and Discussion

For each system (PSBR240k, PSBR14125, PSBR240k/PSBR14125) and for each solvent (bromobenzene, 4-bromo-α-methylbenzyl alcohol) we show three curves. These contain the orientation angle χ as a function of the reduced shear rate β_n, the polymer contribution to the birefringence Δn_1 and, in the same plots, the solvent birefringence Δn_2, both as functions of the shear rate $\dot{\gamma}$, and finally, the orientation resistance m_τ^0 as a function of the concentration c_p.

For our purpose, namely the determination of the intrinsic orientation resistance m_τ^0, the orientation angle must be measured at as small as possible reduced shear rate values. The lowest β_n values shown in Figures 3−5 for the case of bromobenzene or in Figures 6−8 for the case of 4-bromo-α-methylbenzyl alcohol must be considered as lower experimental limits where the birefringence becomes so small that the orientation angles cannot be measured to within satisfactory accuracy.

We can see from Figures 3 and 9, where in the first case the β_n-dependence of the orientation angle and in the second case the $\dot{\gamma}$-dependence of the birefringence

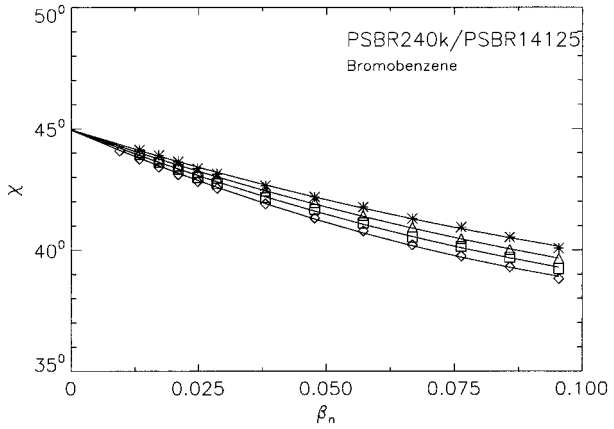

Figure 5. Orientation angle χ as a function of the reduced average shear rate β_n for polystyrene PSBR240k/PSBR14125 in bromobenzene at the concentrations 1.25 (◇), 1.00 (□), 0.75 (△), and 0.50 g/100 mL (∗). All values are corrected according to eq 13.

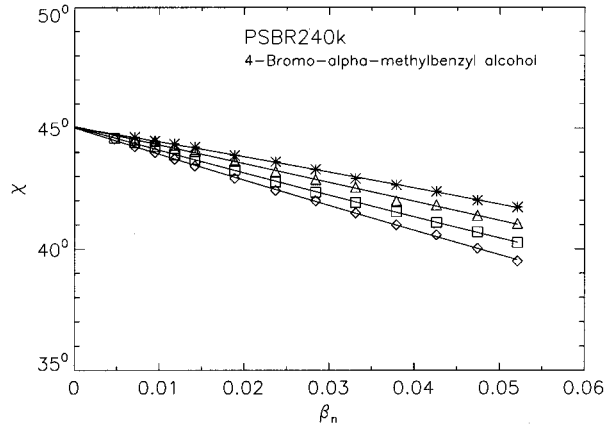

Figure 6. Orientation angle χ as a function of the reduced number average shear rate β_n for polystyrene PSBR240k in 4-bromo-α-methylbenzyl alcohol at the concentrations 2.00 (◇), 1.75, (□), 1.50 (△), and 1.25 g/100 mL (∗). All values are corrected according to eq 13.

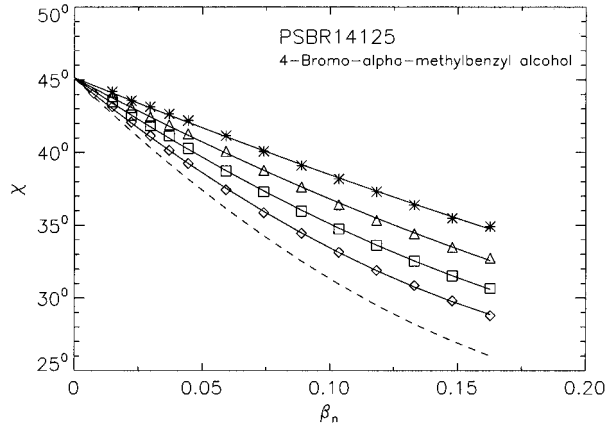

Figure 7. Orientation angle χ as a function of the reduced average shear rate β_n for polystyrene PSBR14125 in 4-bromo-α-methylbenzyl alcohol at the concentrations 1.75 (◇), 1.50 (□), 1.25 (△), and 1.00 g/100 mL (∗). All values are corrected according to eq 13. The uncorrected values for the highest concentration are plotted as a dashed line.

is shown, that although the reduced shear rates β_n are smaller than one, the applied shear rates are high in the sense that they are the highest values obtainable with our apparatus (in the case of bromobenzene $\dot{\gamma} \simeq 12\,000\ s^{-1}$). The characteristic relaxation time scale $\tilde{\lambda} = \langle\langle[\eta]_0\rangle\rangle\eta_s M_n/RT$ of our polymer systems in the solvents

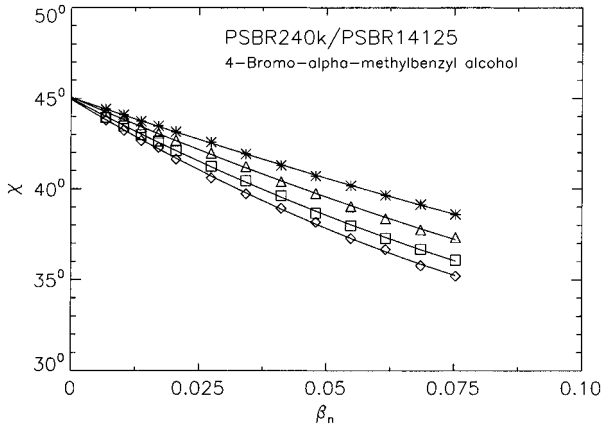

Figure 8. Orientation angle χ as a function of the reduced average shear rate β_n for polystyrene PSBR240k/PSBR14125 in 4-bromo-α-methylbenzyl alcohol at the concentrations 2.00 (◇), 1.75 (□), 1.50 (△), and 1.25 g/100 mL (∗). All values are corrected according to eq 13.

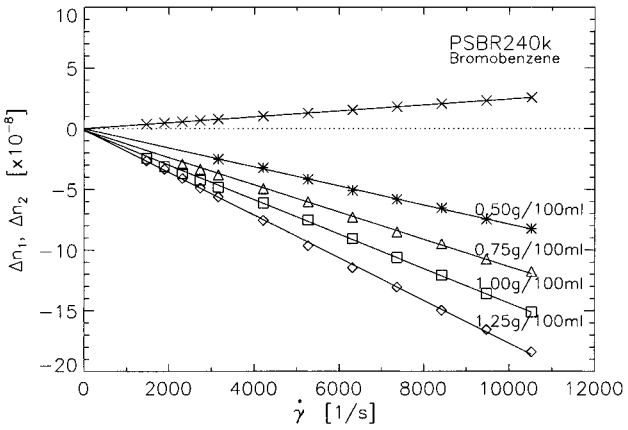

Figure 9. Flow birefringence Δn_1 of the polymer contribution (PSBR240k) for the indicated concentrations and Δn_2 of the pure solvent bromobenzene.

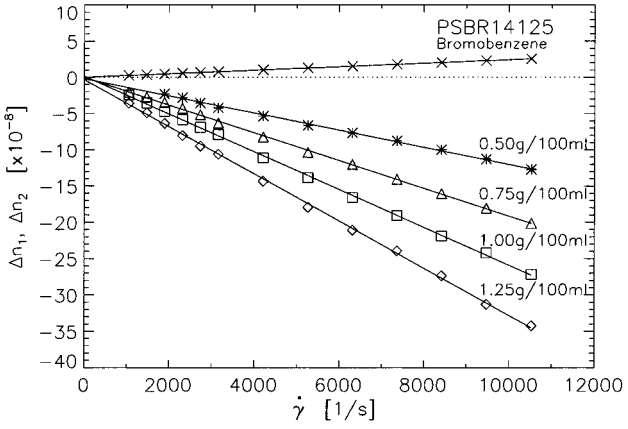

Figure 10. Flow birefringence Δn_1 of the polymer contribution (PSBR14125) for the indicated concentrations and Δn_2 of the pure solvent bromobenzene.

bromobenzene and 4-bromo-α-methylbenzyl alcohol are on the order of $\tilde{\lambda} \simeq 10^{-5}$ s. Very high shear rates, $\dot{\gamma} \simeq 10^5$ s^{-1}, are therefore needed to activate polymer motion on this time scale. A typical value for the applied shear rates is $\dot{\gamma} = 5000$ s^{-1} in the case of bromobenzene (Figures 9−11) and $\dot{\gamma} = 1500$ s^{-1} in the case of 4-bromo-α-methylbenzyl alcohol (Figures 12−14). By choosing higher molecular weights, one can increase the two factors M_n and $\langle\langle[\eta]_0\rangle\rangle$ in the expression for the characteristic relaxation time. Additionally, one can take a

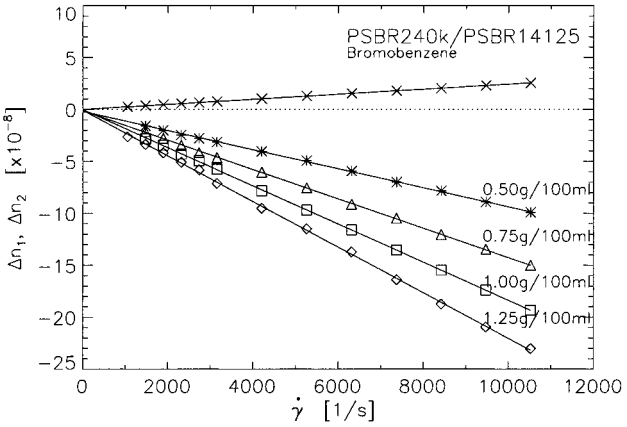

Figure 11. Flow birefringence Δn_1 of the polymer contribution (PSBR240k/PSBR14125) for the indicated concentrations and Δn_2 of the pure solvent bromobenzene.

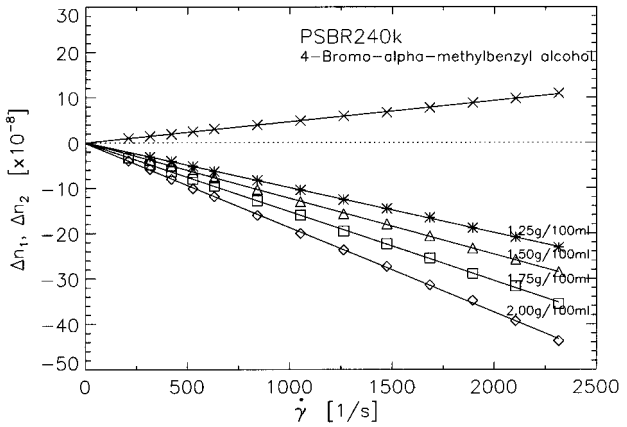

Figure 12. Flow birefringence Δn_1 of the polymer contribution (PSBR240k) for the indicated concentrations and Δn_2 of the pure solvent 4-bromo-α-methylbenzyl alcohol.

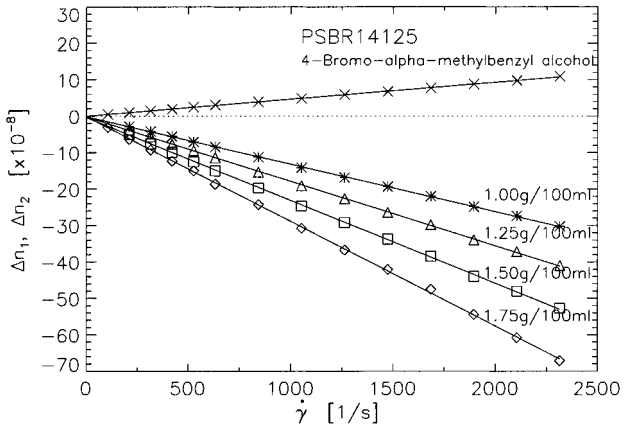

Figure 13. Flow birefringence Δn_1 of the polymer contribution (PSBR14125) for the indicated concentrations and Δn_2 of the pure solvent 4-bromo-α-methylbenzyl alcohol.

high-viscosity solvent such as 4-bromo-α-methylbenzyl alcohol in order to shift the characteristic time scale to larger values if this is desired. If we combine for example the solvent 4-bromo-α-methylbenzyl alcohol with a narrowly distributed polystyrene sample with molecular weight $M_n \simeq 10^7$, which can be synthesized by anionic polymerization, the characteristic time can be estimated by using the Mark Houwink relation with the exponent $a = 0.5$ to be $\tilde{\lambda} \simeq 10^{-2}$ s. With such a combination, high β values can be obtained. Note however, that such high M_w polymer systems may not be used to determine the intrinsic orientation resistance

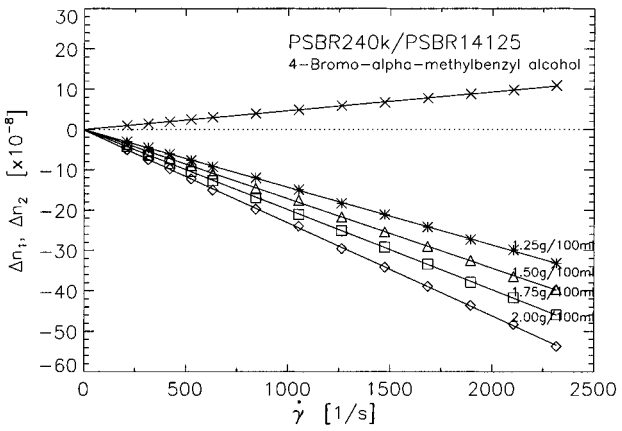

Figure 14. Flow birefringence Δn_1 of the polymer contribution (PSBR240k/PSBR14125) for the indicated concentrations and Δn_2 of the pure solvent 4-bromo-α-methylbenzyl alcohol.

because of the large measurement error arising at small shear rates for systems with high molecular weights (see section 3.2).

We next address another problem occurring at high shear rates: flow instabilities. It can be shown[24] that Taylor instabilities are expected to occur at roughly $\dot{\gamma} \simeq 5,000\ s^{-1}$ in the case of bromobenzene and $\dot{\gamma} \simeq 85\,000\ s^{-1}$ in the case of 4-bromo-α-methylbenzyl alcohol. However, it is argued in section 8.6.2 of ref 24 that a small amount of added polymers stabilizes the flow. In fact, the measurements in bromobenzene did not show any pecularity up to $\dot{\gamma} \simeq 12\,000\ s^{-1}$.

Both solvents, especially 4-bromo-α-methylbenzyl alcohol, have a rather high proper flow birefringence as can be seen, for example, from Figures 9 and 10. It is therefore crucial to understand the influence of the solvent birefringence on the orientation angle measurements and to correct the experimental results (χ,Δn) according to eqs 13 and 14. For that purpose we also have to measure the flow birefringence of the pure solvents ($\chi_2 = \pi/4$, Δn_2). The negative sign of the polystyrene contribution to the birefringence, Δn_1, means that the smaller index of refraction is located in the direction of extinction, which forms an acute angle with the direction of flow. This is due to the fact that the phenyl groups are arranged perpendicularly to the main chain.

We find for all investigated samples a linear dependence between the flow birefringence and the shear rate, which is in accordance with kinetic theory. The orientation angle curves shown in Figures 3−8 are all corrected for the influence of solvent flow birefringence. In order to have an idea of the importance of this correction we plotted in Figures 4 and 7 the original, uncorrected orientation angle curves for the highest concentrations as dashed lines.

For each polymer solution four concentrations were measured. The highest concentrations were chosen to be of the same order as the corresponding overlap concentration (see Table 4). The lowest concentration values were chosen such that the birefringence at small shear rates was still high enough to guarantee a satisfactory accuracy.

From all orientation angle curves we can see that the angle starts at 45° as predicted by formula 1. At small shear rates the flow birefringence is obviously large enough to measure orientation angles near 45°. Hence, the molecular weights of the samples were chosen reasonably.

Measurements in both solvents come closest to 45° for the polymer PSBR240k (see Figures 3−8). This can be understood with the help of formula 8: for a fixed value of the reduced shear rate β_n the birefringence decreases inversely proportional to the molecular weight of the polymers. Hence, since the molecular weight of PSBR240k is the smallest of all samples, the orientation angle measurements can be performed down to lower β values for this polymer system.

The curvature of the orientation angle curves appears to be different for different polymer systems if e.g. Figure 3 is compared to Figure 4. However, this is mainly due to different scales chosen for the abscissa and the ordinate in different experiments.

The concentration dependence of the orientation angle curves can be understood from a semiempirical relation which takes intermolecular interaction in solutions into account. According to Peterlin,[28] eq 1 remains valid at small shear rates if the reduced shear rate β is replaced by its generalization to nonvanishing concentrations $\beta^* = \eta_p M\dot{\gamma}/(c_p RT)$. Equation 1 to first order in the concentration c_p then becomes

$$\tan 2\chi = \frac{m_\tau^0}{\beta}(1 - k_H[\eta]c_p) \tag{15}$$

where k_H is the Huggins constant independent of molecular weight. This equation explains why at a fixed value of β the orientation angle value decreases for increasing concentration, as can be seen from Figure 7 in a rather pronounced form. The increase of flow birefringence Δn_1 with increasing concentration can be understood similarly (see, e.g., ref 2).

In order to obtain the orientation resistance values from the orientation angle and the flow birefringence curves, the following steps have to be performed with the help of eq 3.

In the first step, we calculate the slopes s_τ of the straight lines connecting 45° on the ordinate with the individual shear-rate-dependent orientation angles:

$$s_\tau = \frac{\frac{\pi}{4} - \chi}{\beta_n} \tag{16}$$

The extrapolation to zero shear rate $\beta_n \rightarrow 0$ is performed by fitting polynominals (e.g. with the program TEXTRA[25]) to the s_τ values.

In a second step the resulting orientation resistance values for each concentration have to be extrapolated to zero concentration. We use for that purpose the following expression:

$$m_\tau^{poly}[c_p] = m_\tau^{poly}\exp[-c_p m_\tau^{poly} k] \tag{17}$$

The quantities m_τ^{poly} and k are considered as fit parameters. This ansatz is well-known as the Martin equation for fitting viscosity data, and its utility is widely recognized.[29] As in the case of fitting viscosity data we assume the parameter k to depend only on the solvent quality but to be independent of the molecular weight of the polymers. The resulting m_τ^{poly}-values are displayed in Table 6 and the fits are shown in Figures 15−17 for the solvent bromobenzene and Figures 18−20 for 4-bromo-α-methylbenzyl alcohol.

In Figure 16 (PSBR14125 in bromobenzene), the exponential curve does not seem to fit the experimental values very well. Indeed, a simple linear regression

Table 6. Orientation Resistance and Its Measurement Error for the Polydisperse Polystyrene Samples and the Corresponding Monodisperse Values Calculated with the Help of the Polydispersity Factors Displayed in Table 5[a]

	bromobenzene				4-bromo-α-methylbenzyl alcohol			
	m_τ^{poly}	Δm_τ^{poly}	m_τ^{mono}	Δm_τ^{mono}	Δm_τ^{mono}	Δm_τ^{poly}	m_τ^{mono}	Δm_τ^{mono}
PSBR240k	0.91	0.13	**3.70**	**0.53**	1.09	0.27	**3.20**	**0.79**
PSBR14125	1.06	0.13	**3.93**	**0.48**	1.10	0.24	**3.14**	**0.69**
PSBR240k/PSBR14125	0.64	0.08	**3.58**	**0.45**	0.80	0.19	**3.04**	**0.72**

[a] By Δm_τ^{poly} we denote the total error in the polydisperse orientation resistance and by Δm_τ^{mono}, the total error in the monodisperse orientation resistance measured with flow birefringence.

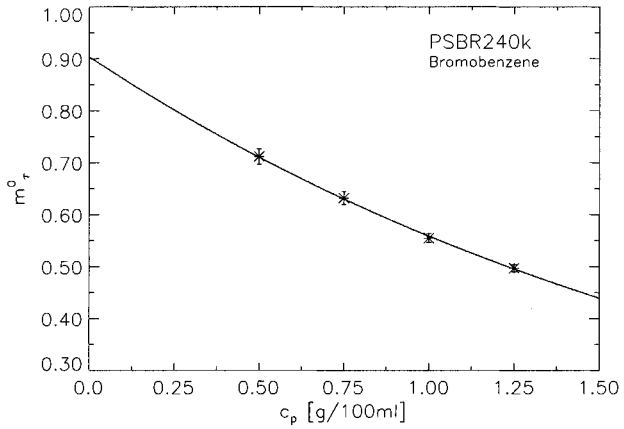

Figure 15. Extrapolation of the orientation resistance m_τ^0 of PSBR240k for $c_p \rightarrow 0$ in bromobenzene. The error bars indicate the statistical errors arising from the orientation angle measurements after extrapolating the m_τ^0-values to $\beta \rightarrow 0$ for each concentration.

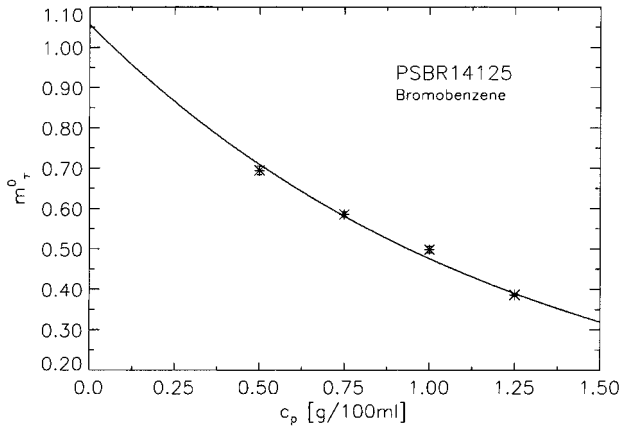

Figure 16. Extrapolation of the orientation resistance m_τ^0 of PSBR14125 for $c_p \rightarrow 0$ in bromobenzene. The error bars indicate the statistical errors arising from the orientation angle measurements after extrapolating the m_τ^0-values to $\beta \rightarrow 0$ for each concentration.

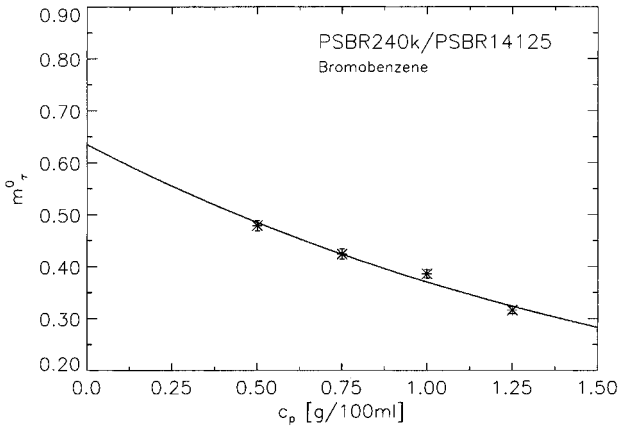

Figure 17. Extrapolation of the orientation resistance m_τ^0 of PSBR240k/PSBR14125 for $c_p \rightarrow 0$ in bromobenzene. The error bars indicate the statistical errors arising from the orientation angle measurements after extrapolating the m_τ^0-values to $\beta \rightarrow 0$ for each concentration.

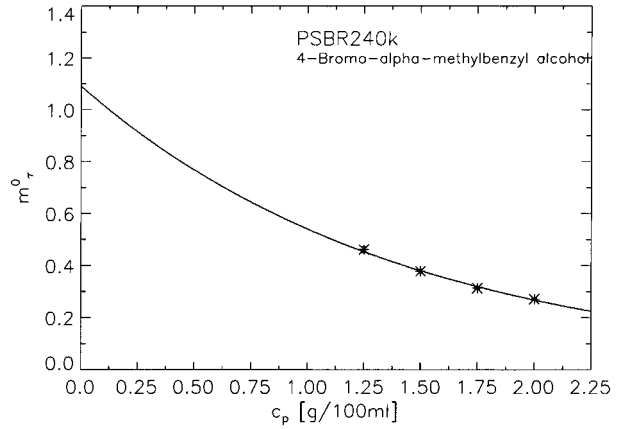

Figure 18. Extrapolation of the orientation resistance m_τ^0 of PSBR240k for $c_p \rightarrow 0$ in 4-bromo-α-methylbenzyl alcohol. The error bars indicate the statistical errors arising from the orientation angle measurements after extrapolating the m_τ^0-values to $\beta \rightarrow 0$ for each concentration.

would better fit the data. The extrapolated orientation resistance would then be $m_\tau^{poly} = 0.90 \pm 0.01$ or $m_\tau^{mono} = 3.33 \pm 0.04$. However, Martin-type equations are widely used and tested. Since the exponential curves fit properly to the experimental data of the other samples, we assume the same fit to be valid for PSBR14125 in bromobenzene as well. As can be seen from Table 6, the extrapolated orientation resistance value is considerably higher when fitted with an exponential function instead of a linear one. The same is true for the measurement error. A comparison of Δm_χ^{stat} in Table 7 to the above quoted error for the linear fit reveals that the error for the exponential fit is twice as large.

For a discussion of the results, the magnitude of the errors must be considered. A detailed explanation of the error analysis can be found in the Appendix. We split the total error in a systematic and statistic part, where we take into account a systematic and a statistic error in reading the orientation angle, Δm_χ^{syst} and Δm_χ^{stat}, a statistic error in the reduced shear rate, Δm_β^{stat}, and a statistic error in the concentration, $\Delta m_{c_p}^{stat}$. In Table 7 we can see that the error Δm_β^{stat} is greater than the other errors, especially in the case of 4-bromo-α-methylbenzyl alcohol. However, it is in fact not Δm_β^{stat} that deals with the flow birefringence experiment itself but the errors in reading (Δm_χ^{stat}, Δm_χ^{syst}) and the errors coming from the preparation of the individual concentrations ($\Delta m_{c_p}^{stat}$). We call the total error in absence of Δm_β^{stat} the operational error, which is much smaller than the total error Δm_τ^{poly}

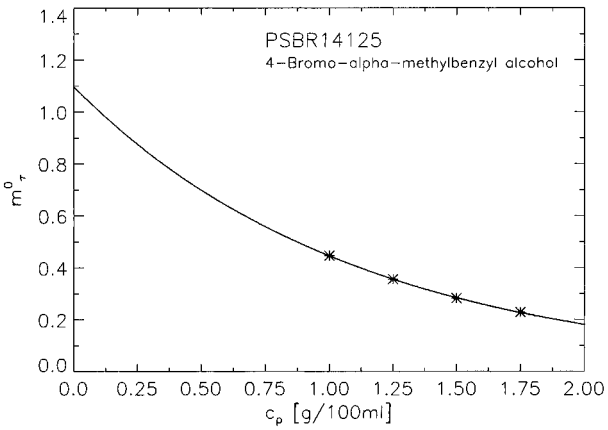

Figure 19. Extrapolation of the orientation resistance m_τ^0 of PSBR14125 for $c_p \rightarrow 0$ in 4-bromo-α-methylbenzyl alcohol. The error bars indicate the statistical errors arising from the orientation angle measurements after extrapolating the m_τ^0-values to $\beta \rightarrow 0$ for each concentration.

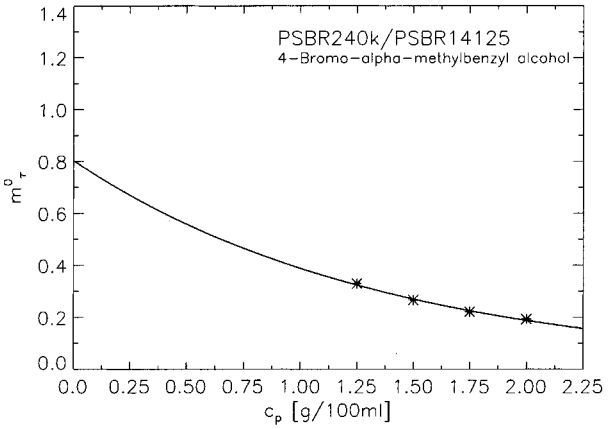

Figure 20. Extrapolation of the orientation resistance m_τ^0 of PSBR240k/PSBR14125 for $c_p \rightarrow 0$ in 4-bromo-α-methylbenzyl alcohol. The error bars indicate the statistical errors arising from the orientation angle measurements after extrapolating the m_τ^0-values to $\beta \rightarrow 0$ for each concentration.

Table 7. Statistical (stat) and Systematical (syst) Measurement Errors in the Orientation Resistance Coming from the Orientation Angle Measurement (χ), from the Uncertainty in the Concentration (c_p) and in the Reduced Shear Rate β[a]

	bromobenzene				
	Δm_χ^{stat}	$\Delta m_{c_p}^{stat}$	Δm_β^{stat}	Δm_χ^{syst}	Δm_τ^{poly}
PSBR240k	0.03	0.02	0.09	0.03	0.13
PSBR14125	0.02	0.04	0.11	0.01	0.13
PSBR240k/PSBR14125	0.02	0.02	0.06	0.01	0.08
	4-bromo-α-methylbenzyl alcohol				
	Δm_χ^{stat}	$\Delta m_{c_p}^{stat}$	Δm_β^{stat}	Δm_χ^{syst}	Δm_τ^{poly}
PSBR240k	0.06	0.04	0.22	0.04	0.27
PSBR14125	0.03	0.05	0.22	0.01	0.24
PSBR240k/PSBR14125	0.03	0.03	0.16	0.02	0.19

[a] In the last column, Δm_τ^{poly} denotes the total error.

indicated in Table 7. Indeed, the error Δm_β^{stat} depends strongly on how accurate the molecular mass distribution is known because as we saw above the errors in the viscosity and the intrinsic viscosity measurement are negligible if an automatic capillary viscometer is used. Since we treated the errors in Δm_β^{stat}, namely the error in the average molecular weight and in the intrinsic viscosity measurement, as statistical errors one could ask why these measurements were not repeated as many times as necessary to make the errors smaller. The reason is that the actual error includes systematic errors as well, and it is difficult to distinguish between statistical and systematic errors in these measurements. It is for convenience that we treat the whole error as a statistical one. Repeated GPC and intrinsic viscosity measurements would therefore only partially reduce the error Δm_β^{stat}, and the estimate of the error would be as difficult as it is now. However, an automatic capillary viscometer constructed for high-viscosity solutions such as 4-bromo-α-methylbenzyl alcohol would certainly reduce the error in the intrinsic viscosity considerably.

With the help of the polydispersity factors in Table 5 the measured orientation resistance values and the corresponding errors can be transformed to monodisperse quantities (see Table 6). If we compare the orientation resistance results for the two solvents separately among each other, we notice a nearly perfect agreement, proving the validity of our treatment of the polydispersity. Due to the small operational error we can interpret this result as a success for the birefringence method.

Comparing the monodisperse values of Table 6 with our theoretical values displayed in Table 1 we can see that the value calculated in the framework of the Gaussian approximation coincides best with the experimental values in bromobenzene whereas in the case of 4-bromo-α-methylbenzyl alcohol the values fit to the renormalization group result. The Gaussian approximation result, however, is the value that fits best to the experimental results in both solvents within the indicated error bars. The experimental deviation between the values for the two solvents can be explained by the assumption of a good solvent ($\nu = 0.588$) and a Θ solvent ($\nu = 0.5$) in the correction procedure of polydispersity. Neither can bromobenzene be considered as a perfectly good solvent nor can 4-bromo-α-methylbenzyl alcohol actually be considered as a Θ solvent; i.e. the polydispersity factors for the polymer systems in bromobenzene should probably be a little higher than the indicated values and the ones for the systems in 4-bromo-α-methylbenzyl alcohol a little lower. This can be the reason why the monodisperse orientation resistance values in bromobenzene are higher than the ones in 4-bromo-α-methylbenzyl alcohol.

The individual results displayed in Table 6 are calculated from statistical independent measurements. In order to identify one orientation resistance value for each solvent and to reduce the measurement error, we determined the arithmetic mean of the values in Table 6. We obtained $m_\tau^0 = 3.74 \pm 0.28$ in the case of bromobenzene and $m_\tau^0 = 3.13 \pm 0.42$ in the case of 4-bromo-α-methylbenzyl alcohol.

One could ask now whether the polydispersity of the mixture differs enough from the one of the two individual components. Is the polydispersity effect really measurable in the sense that it exceeds the error? From the polydisperse orientation resistance values and the corresponding errors in Table 6, we conclude that the mixture we used indeed produces a measurable polydispersity effect.

Finally, we give an example to illustrate the accuracy of the presented flow birefringence method for the determination of molecular weights. Let us assume that the monodisperse orientation resistance m_τ^0 is known exactly by choosing, for example, the value obtained from the Gaussian approximation or from the renormalization group procedure presented in Table 1. We

Table 8. Orientation Resistance Values Recalculated from Experimental Results of the Indicated Publications[a]

polymer	solvent	$10^{-6}M$	m_τ^0
(1) polystyrene[2]	toluene	0.45−1.9	0.59
	methyl ethyl ketone	0.45−1.9	0.50
(2) polystyrene[2]	benzene	0.9−5.2	1.52
(3) polystyrene[2]	bromoform	0.57−4.3	1.56
(4) polystyrene[31]	bromobenzene	1.59 ($w \leq 1.09$)	2.70
(5) polystyrene[32]	bromobenzene	0.27 ($w = 1.52$)	1.43
(6) polystyrene[3]	4-bromo-α-methyl-benzyl alcohol	0.23	4.34

[a] The molecular weight (M) data are taken directly from refs 2, 3, 31, and 32.

then assume that we will investigate the orientation angle χ of a polymer system in solution, such as polystyrene in bromobenzene, with an a priori known type of molecular weight distribution. We want to see now, how accurate the number-average molecular weight can be determined from our orientation angle measurements. From these assumptions, the orientation resistance of the investigated sample arising from eq 5 is known exactly. The only source of errors in the determination of M_n are the statistical and systematic errors in reading the angle χ and the error coming from the preparation of the individual concentrations. From the measurement errors in the slopes s_τ extrapolated to zero concentration we can determine the relative error $\Delta M_n/M_n$.[24]

From our results shown in Table 7 for PSBR14125 and PSBR240k in bromobenzene we obtain relative errors of 3% and of 4%, respectively. This is a remarkable result. It underlines the accuracy of flow birefringence and indicates that it is a very precise method for determining molecular weights, probably more precise than any other known standard method such as GPC, light scattering, or osmotic pressure. Furthermore, it shows how important it is to have a reliable value for the orientation resistance m_τ^0 as it is provided by the Gaussian approximation or by the renormalization group treatment.

Reliable flow birefringence experiments in steady shear flow date from the 1960s. In that period the experimental technique was established.[2,3] In Table 8 we present values for the orientation resistance recalculated from original data in Tsvetkov's review[2] and Janeschitz-Kriegl's paper.[3] In Tsvetkov's review the orientation resistances are calculated by plotting the initial slopes of the orientation angle curves (as functions of $\dot\gamma$) for different weight fractions of the polydisperse samples versus $M\eta_s\langle\langle[\eta]_0\rangle\rangle$. This relationship is linear and from the slope of the curve the orientation resistance can be read off. The molecular weight values in runs 4 and 5 in Table 8 are number-average molecular weights. Sample 6 is assumed to be very narrowly distributed.

Obviously, the individual orientation resistance values strongly differ from each other. The discrepancy between the individual orientation resistance values are interpreted by Tsvetkov to be manifestations of "structural peculiarities of the polymer-solvent systems studied, or are due to experimental errors". From the molecular weight data in Table 8, we can instead deduce that all the samples investigated by Tsvetkov are polydisperse to some extent. Neither the polydispersity nor the influence of the solvent birefringence on the orientation resistance was taken into account in that work. We note that the orientation resistance value for the nearly monodisperse system 6, namely $m_\tau^0 = 4.34$, is much higher than all the other values for the polydisperse systems.

While for bromoform, toluene, and benzene form birefringence can be neglected, this is not the case for methyl ethyl ketone, which has an index of refraction that is rather different from the one of polystyrene, and form birefringence certainly plays a role in the orientation angle measurements. Form birefringence was investigated experimentally in refs 2 and 3. It was found in ref 3 that with polystyrene in dioxane where the intrinsic anisotropy of polystyrene is negative, form birefringence counteracts the effect caused by the intrinsic anisotropy of the random links and that the initial slope of the unperturbed extinction angle curve is increased. It can be inferred from these experimental findings that the orientation resistance is reduced in the case of polystyrene when form birefringence becomes important, so that the very low orientation resistance value in Table 8 in the case of methyl ethyl ketone can probably be associated with form birefringence.

From a theoretical viewpoint form birefringence is a complicated effect. It is directly related to the anisotropy in the structure factor, which has not yet been calculated in a closed form in the framework of kinetic theory with the approximations discussed in section 2.2.

Obviously, a direct comparison to existing data is difficult because polydispersity, solvent birefringence and form birefringence have not all been taken seriously into account in previous works. However, we can see that all orientation resistances originating from polydisperse samples in Table 8 are clearly lower than our theoretical and experimental monodisperse values.

The strong sensitivity of this method to polydispersity motivates the usage of flow birefringence for the determination of molecular weight distributions of polymers. The shear rate dependence of the orientation resistance plays a decisive role in that idea. We follow the picture that with each shear rate value (a reciprocal time) a particular characteristic time and therefore a certain molecular weight of the polymer system is activated. Covering a large shear rate domain allows us to scan the corresponding molecular weight range of the polymer system under consideration. In a similar spirit the dynamic storage and loss moduli of polymer melts are used in rheology to determine molecular weight distributions.[33] The flow birefringence method for dilute solutions however has a great advantage. Whereas for polymer melts the individual chains are interacting with each other and, therefore, the mixing rules can only be guessed by using model predictions, the situation is much simpler for polymer solutions. The mixing rule can be written down directly[1,24]

$$\langle\langle m_\tau(\beta)\rangle\rangle = \beta_n \frac{2\langle\langle\tau_{12}(\beta)\rangle\rangle_n}{\langle\langle\tau_{11}(\beta) - \tau_{22}(\beta)\rangle\rangle_n} \tag{18}$$

Here, $\langle\langle m_\tau(\beta)\rangle\rangle$ is the measured polydisperse orientation resistance. A monodisperse gauge curve $m_\tau(\beta)$ together with a second measuring curve, for example the shear-rate-dependent viscosity, contain enough information to invert relation 18 numerically. At very small and very large shear rates $\dot\gamma$ scaling laws for the stress tensor (see refs 1 for low and ref 34 for high shear rates) can be used as boundary conditions for the inversion of eq 18. The inversion of equation 18 with the aim of getting out the molecular weight distribution is an ill-posed

problem[35] and must be treated with a regularization method or the maximum entropy method.

In determining the monodisperse gauge curve $m_\tau(\beta)$, one should of course try to achieve as high as possible values for the reduced shear rate β. This means that, apart from a high $\dot{\gamma}$, the molecular weight of the polymers and the viscosity of the solvent must be large. Certainly, at large molecular weights the precision of the orientation angle measurement is lowered at very low shear rates; however, as we have seen, there is no need for a numerical inversion process at very low shear rates. At higher shear rates the precision should be good enough even for large molecular weights.

A large solvent viscosity produces large torques on the driving shaft at high shear rates $\dot{\gamma}$. The driving shaft in our rotor unit was made of a very thin steel axis in order to keep the heat loss low. A new construction of the unit should involve a driving shaft made for example of fiber-reinforced plastic material as it can be obtained from the filament winding process in which the continuous fiber reinforcements are wound over a rotating mandrel. The wind angle should be for our purpose "near hoop" relative to the mandrel axis, since the load on the driving shaft of our apparatus is a pure torsional one. The main advantage of filament winding is that fiber contents of 60−85% may be attained, making possible exceptionally high strength especially in the direction of the filament orientation.[36] Such parts are for example successfully used for automotive driving shafts. With that idea, both problems, the heat loss as well as the resistance against high torques, can be solved.

The most important experimental problem however arises with the choice of the solvent. A solvent which fulfills practically all requirements can certainly be found for polystyrene with a nearly vanishing refractive index increment. We came across two examples and others could be found by mixing individual components. The form birefringence however constitutes a serious problem for polymers that do not have such a large variety of solvents; most likely then the available solvents fulfilling the other requirements have a refractive index different from the one of the polymer. Since the validity of the stress−optical law is assumed in the above mixing rule, form birefringence has either to be avoided or a suitable way must be found to correct the results properly for this effect. Form birefringence is directly related to the structure factor, which can in principle be determined by light scattering, neutron scattering, or X-ray scattering. By a combination of, for example, light scattering and neutron scattering, the whole $\boldsymbol{q}$-range could be covered, which is necessary in the calculation of form birefringence. Then, form birefringence could be subtracted from the measured flow birefringence. In section 2.1 we mentioned that intrinsic birefringence and form birefringence are supposed to be additive. With this point in mind one could think of adapting the treatment of solvent birefringence in order to correct the orientation angle and hence the orientation resistance for the form birefringence effect.

5. Conclusion

In the present work the orientational behavior of polymers in dilute solutions undergoing shear flow was investigated experimentally by flow birefringence and compared to theory. The main interest was not focused on the orientation angle of the polymers itself but on the orientation resistance, which is a universal quantity in the limit of vanishing shear rate. This intrinsic orientation resistance characterizes the orientational behavior of polymers at low shear rates. It was found theoretically[1] that this quantity strongly depends on the polydispersity of polymer samples.

With our measurements we could determine the intrinsic orientation resistance in a good and a Θ solvent with a high precision. This was on the one hand possible due to a thorough construction of the rotor unit (from the original apparatus of H. Janeschitz-Kriegl) allowing measurements of orientation angles even at small flow birefringences of the order of $\Delta n = 10^{-8}$. On the other hand we chose the solvents to be nearly isorefractive with polystyrene and corrected the results for the influence of the solvent birefringence. Two radical polymerized polystyrene samples with different molecular weights were measured. After a careful error analysis, the obtained values for the polydisperse orientation resistance were corrected for polydispersity by means of a procedure given by theory. The values in the Θ solvent are slightly lower than the ones in the good solvent. However, it is argued that this discrepancy cannot be associated with the experiments but rather with the assumptions made about the quality of the solvents. The errors involved in the determination of the orientation resistance from orientation angle measurements are mainly due to errors in the reduced shear rate. The actual operational error turned out to be rather small.

In order to test the predicted sensitivity on polydispersity, we mixed both polystyrene samples. The theoretical polydispersity analysis was proven to be in very good agreement with the experiments. Indeed, the sensitivity is so strong that one could think of using shear-rate-dependent orientation resistance measurements to measure molecular weight distribution functions with this method. It was shown that with flow birefringence molecular weights can be determined with a relative error of only 3%.

The experimental values in the good and the Θ solvent corrected for polydispersity coincide best (within the measurement error) with the monodisperse values obtained in the framework of the Gaussian approximation where hydrodynamic interaction but no excluded volume effect is included. This also proves the neglectable influence of excluded volume on the orientation resistance.

Acknowledgment. The authors are indebted to Professor H. Janeschitz-Kriegl for leaving us his flow birefringence apparatus, for his hospitality during J.B.'s visit to the Johannes Kepler Universität Linz, and for supporting J.B. by many helpful comments during the reinstatement of the apparatus. We greatly appreciate the invaluable help of Jürg Hostettler in adjusting the optical system. We would also like to thank Professor Norman Wagner for reading the article and for his helpful comments. Financial support from the Swiss National Foundation for Scientific Research (Grant No. 20-36073.92) is gratefully acknowledged.

Appendix: Error Analysis

The errors arising in the reduced shear rate β_n and in the concentration c_p are included only after the extrapolation of the slope s_τ to zero shear rate and after the subsequent concentration extrapolation with eq 17.

In these extrapolation procedures a statistical error in reading the orientation angle of $\pm^1/_{10}$ degree is considered, leading to the statistical error in reading, $\Delta m_\chi^{\text{stat}}$, displayed in Table 7.

The error in the reduced shear rate β_n comes from the errors in the measurements of the intrinsic viscosity $\langle\langle[\eta]_0\rangle\rangle$ and the number-average molecular weights M_n. The potential error in the viscosity data is supposed to be very small and negligible. The intrinsic viscosities of the three samples in bromobenzene were measured with an automatic capillary viscometer (see section 3.2). The measuring error can also be neglected in this case. The error in the intrinsic viscosity of the samples in 4-bromo-α-methylbenzyl alcohol of about 10% is treated as a statistical error. The average molecular weights are determined by GPC. Now, the total errors of the average molecular weights M_n have various origins such that again we interpret them as statistical errors and we estimate them to be 10% of the respective molecular weight values. The resulting errors $\Delta m_\beta^{\text{stat}} = m_\tau^{\text{poly}} \Delta\beta_n/\beta_n$ can be found in Table 7.

The inaccuracy in the preparation of the individual concentrations is also of a statistical nature. We estimate the error to be $\Delta c_p = \pm 0.05$ g/100 mL and calculate the influence on m_τ^0 by the multiplication of Δc_p with the initial slope of the concentration extrapolation curve. The results, $\Delta m_{c_p}^{\text{stat}}$, obtained in this way are displayed in Table 7.

All the statistical errors that we discussed above are now squared and added. The square root of the sum gives the total statistical error. To this error we have to add the systematic error in reading, $\Delta m_\chi^{\text{syst}}$, which comes from a certain subjectivity in the estimate of optimum darkness. We assume a systematic error in reading of $^1/_{10}°$ in the case of 4-bromo-α-methylbenzyl alcohol and $^1/_{20}°$ in the case of bromobenzene. It follows from the nature of the least-squares method that a systematic error which is proportional to the quantity to be extrapolated remains proportional to the extrapolated quantity. We courageously pretend the systematic error to be proportional to the orientation resistance and display the results in Table 7.

The total error $\Delta m_\tau^{\text{poly}}$ of the measurement is then calculated according to the formula

$$\Delta m_\tau^{\text{poly}} = \sqrt{(\Delta m_\chi^{\text{stat}})^2 + (\Delta m_{c_p}^{\text{stat}})^2 + (\Delta m_\beta^{\text{stat}})^2} + \Delta m_\chi^{\text{syst}} \tag{19}$$

and displayed in Tables 6 and 7 for the three polymer systems and the two solvents.

References and Notes

(1) Bossart, J.; Öttinger, H. C. *Macromolecules* **1995**, *28*, 5852.
(2) Tsvetkov, V. N. *Polym. Rev.* **1964**, *6*, 563.
(3) Janeschitz-Kriegl, H. *Adv. Polym. Sci.* **1969**, *6*, 170.
(4) Janeschitz-Kriegl, H. *Polymer Melt Rheology and Flow Birefringence*; Springer: Berlin, 1983.
(5) Kuhn, W.; Kuhn, H. *Helv. Chim. Acta* **1943**, *26*, 1394.
(6) Doi, M.; Edwards, S. F. *The Theory of Polymer Dynamics*; International Series of Monographs on Physics 73; Oxford University Press: Oxford, England, 1992.
(7) Čopič, M. *J. Chem. Phys.* **1957**, *26*, 1382.
(8) Frisman, E. V.; Tsvetkov, V. N. *J. Polym. Sci.* **1958**, *30*, 297.
(9) Dinkel, A. Beziehungen zwischen Orientierung, optischen und mechanischen Eigenschaften von Polystyrol im flüssigen und festen Zustand. Ph.D. Thesis 9640, ETH Zürich, 1992.
(10) Bird, R. B.; Curtiss, C. F.; Armstrong, R. C.; Hassager, O. *Dynamics of Polymeric Liquids. Kinetic Theory*, 2nd ed.; Wiley-Interscience: New York, 1987; Vol. 2.
(11) Rouse, P. E. *J. Chem. Phys.* **1953**, *21*, 1272.
(12) Zimm, B. H. *J. Chem. Phys.* **1956**, *24*, 269. A corrected version of that paper can be found in: Hermans, J. J. *Polymer Solutions Properties, Part II: Hydrodynamics and Light Scattering*; Dowden, Hutchinson and Ross: Stroudsburg, PA, 1978; pp 73−84. For corrections to Zimm's paper, see also: Williams, M. C. *J. Chem. Phys.* **1965**, *42*, 2988; **1965**, *43*, 4542.
(13) Öttinger, H. C. *J. Chem. Phys.* **1987**, *86*, 3731.
(14) Öttinger, H. C. *J. Chem. Phys.* **1989**, *90*, 463.
(15) Wedgewood, L. E. *J. Non-Newtonian Fluid Mech.* **1989**, *31*, 127.
(16) Öttinger, H. C.; Rabin, Y. *J. Non-Newtonian Fluid Mech.* **1989**, *33*, 53.
(17) Öttinger, H. C. *Phys. Rev. A* **1989**, *40*, 2664.
(18) Van Kuik-Van Meerten, E.; Janeschitz-Kriegl, H. *J. Sci. Instrum.* **1962**, *39*, 301.
(19) Janeschitz-Kriegl, H. *Rev. Sci. Instrum.* **1960**, *31*, 119.
(20) Janeschitz-Kriegl, H. *Physica* **1958**, *24*, 913.
(21) Janeschitz-Kriegl, H.; Nauta, R. *J. Sci. Instrum.* **1965**, *42*, 880.
(22) Janeschitz-Kriegl, H. *J. Polym. Sci.* **1957**, *23*, 181.
(23) Janeschitz-Kriegl, H. *Physica* **1956**, *22*, 1197.
(24) Bossart, J. Polymer orientation in dilute solutions undergoing shear flow: a theoretical and experimental approach. Ph.D. Thesis 12085, ETH Zürich, 1997.
(25) Öttinger, H. C. *Stochastic Processes in Polymeric Fluids*; Springer: Berlin, 1996.
(26) Szivessy, G. In *Handbuch der Physik*; Konen, H., Ed.; Springer Verlag: Berlin, 1928; Vol. 19.
(27) Sadron, Ch. *J. Phys.* **1938**, *9*, 381.
(28) Peterlin, A. *J. Polym. Sci.* **1954**, *12*, 45.
(29) Manke C. W.; Williams M. C. *J. Non-Newtonian Fluid Mech.* **1985**, *19*, 43.
(30) Brandrup J.; Immergut E. H. *Polymer Handbook*; Wiley-Interscience: New York, 1989.
(31) Janeschitz-Kriegl, H. *Kolloid Z. Z. Polym.* **1965**, *203*, 119.
(32) Janeschitz-Kriegl, H.; Henrici-Olivé, G.; Olivé, S. *Kolloid Z. Z. Polym.* **1963**, *191*, 97.
(33) Wasserman, S. H.; Graessley, W. W. *J. Rheol.* **1992**, *36*, 543.
(34) Öttinger, H. C. *Phys. Rev. A* **1990**, *41*, 4413.
(35) Honerkamp, J. *Rheol. Acta* **1989**, *28*, 363.
(36) Hull, D. *An Introduction to Composite Materials*; Cambridge Solid State Science Series; Cambridge University Press: Cambridge, England, 1981.

MA970328L